Supporting Information

Daptomycin inhibits cell envelope synthesis by interfering with fluid membrane microdomains

Anna Müller, Michaela Wenzel, Henrik Strahl, Fabian Grein, Terrens N. V. Saaki, Bastian Kohl, Tjalling Siersma, Julia E. Bandow, Hans-Georg Sahl, Tanja Schneider, Leendert W. Hamoen

Supporting Methods

Supporting Table 1: *Bacillus subtilis* strains used in this study

Supporting Table 2: Plasmids used in this study

Supporting Table 3: Primers used in this study

Supporting Figure 1: Effect of daptomycin on macromolecule synthesis

Supporting Figure 2: Influence of daptomycin on energy metabolism and cell growth

Supporting Figure 3: Cell permeability assay using propidium iodide

Supporting Figure 4: Effect of daptomycin on membrane lipids

Supporting Figure 5: Overview pictures of DiIC12-stained membrane patches

Supporting Figure 6: Overview pictures of colocalization of DiIC12 with daptomycin-BODIPY in cells pre-treated with benzyl alcohol

Supporting Figure 7: Overview of the effects of different cell envelope-targeting antibiotics on the membrane of *B. subtilis*

Supporting Figure 8: Line scans of 5 representative cells expressing MurG-GFP before and after 10 minutes treatment with 2 µg/ml daptomycin

Supporting Figure 9: *B. subtilis* after 10 minutes treatment with 1 µg/ml daptomycin and 3 µg/ml daptomycin-Bodipy in the absence and presence of 1.25 mM $CaCl_2$

Supporting Figure 10: Daptomycin does not influence the membrane localization of the cell wall synthesis proteins MraY, PBP1, and PBP2

Supporting Figure 11: Membrane fluidity after prolonged daptomycin treatment

Supporting Figure 12: Localization of DivIVA

Supporting Figure 13: Growth experiments for proteome analysis

Supporting Figure 14: MurG-msfGFP is functional

Supporting References

SUPPORTING METHODS

Strain construction

The plasmid pHJS103 used for generating N-terminal fusions with monomeric GFP was constructed from xylose-inducible *amyE*-integration plasmid pSG1729 using the quick-change method and oligonucleotides GFPA206K-for and GFPA206K-rev, thereby rendering GFP monomeric (GFP_{A206K}). The plasmid pMW1 used for generating C-terminal fusions with monomeric superfolder GFP (msfGFP) was constructed by replacing the *gfp*-coding region on a xylose-inducible *amyE*-integration plasmid pSG1154 with *msfgfp* using the Gibson assembly method and DNA-fragments obtained with oligonucleotides MW30/MW31 (vector linearization) and MW32/MW33 (*msfgfp* fragment) [1]. The plasmid pMW1 was further modified with Gibson-assembly of DNA-fragments originating from PCR-amplification of pMW1 with oligonucleotides TerS278/TNVS146 and TerS273/TerS145, thereby yielding plasmid pTNV64. *plsX* was PCR-amplified from *B. subtilis* 168 chromosomal DNA using oligonucleotides PlsX-Fw and PlsX-Re, followed by ligation into *Xho*I/*Eag*I-linearized pHJS103 resulting in plasmid pTNV12 (*Pxyl-plsX-mgfp*). *ponA* was PCR-amplified using oligonucleotides TerS93 and TerS94, followed by ligation into *Eco*RI/*Xho*I-linearized pHJS103 yielding plasmid pTNVS20 (*Pxyl-ponA-mgfp*). *murG* was PCR-amplified with oligonucleotides TerS366 and TerS367, followed by a Gibson-assembly with pTNV64 PCR-linearized into two fragments with oligonucleotides TerS278/TerS146 and TerS273/TerS145 resulting in plasmid pTNV77 (*Pxyl-murG-msfGFP*). The plasmid pTNV95 was created by replacing *msfGFP* coding sequence of pTNV77 with *mCherry* using Gibson assembly. For this aim, *mCherry* was PCR-amplified using oligonucleotides TerS401 and TerS402 and the plasmid pTNV77 using oligonucleotides TerS343/TerS403 and TerS366/TerS340, respectively. A three fragment Gibson assembly with the respective PCR-products yielded the plasmid pTNV95 (*Pxyl-murG-mcherry*). *mraY* was PCR-amplified using oligonucleotides TerS404 and TerS405, followed by a Gibson-assembly with pTNV64 PCR-linearized into two fragments with oligonucleotides TerS278/TNVS146 and TerS273/TerS145 resulting in plasmid pTNV105 (*Pxyl-mraY-msfgfp*). *pbpB* was PCR-amplified using oligonucleotides EKP31 and EKP32, followed by a Gibson-assembly with pHJS105 PCR-linearized with oligonucleotides EKB20 and EKB30 yielding plasmid pEKC12 (*Pxyl-msfgfp-pbpB).* The plasmid pDG7-sfGFP encoding DivIVA-sfGFP was converted into a monomeric superfolder GFP derivative (pDG7-*msfGFP*) using the quick-change method and oligonucleotides HS404/HS405. Followed by sequencing, the plasmids were integrated into *B. subtilis* wild type genome using starvation-induced natural competence [2], followed by selection on 100 µg/ml spectinomycin or 1 µg/ml erythromycin containing plates. The integration into the *amyE*-locus was verified by testing for α-amylase activity on plates supplemented with 1% starch.

To express *murG-msfgfp* from its native locus and by its native promoter, a DNA-fragment containing the 3'-end of *murG* (corresponding to amino acids G193-K363) fused to *msfgfp* was PCR-amplified from plasmid pTNV77 using oligonucleotides TerS371 and TerS372. The resulting PCR-product was fused with pMUTIN4 PCR-linearized with oligonucleotides TerS369 and TerS370 using Gibson assembly. The resulting plasmid was integrated into *B. subtilis murG*-locus thereby replacing the native *murG* with *murG-msfgfp* while maintaining expression of downstream genes with the co-inserted IPTG-inducible *Pspac*-promoter. The ability of the resulting strain to grow and exhibit cell morphology comparable to that of the wild type cells indicates that MurG-msfGFP fusion protein is functional. Furthermore, this fusion protein exhibits localization pattern identical to an ectopic *Pxyl*-driven fusion (Supporting Figure 13).

Antibiotics

Daptomycin was purchased from Novartis, all other antibiotics from Sigma Aldrich, with exception of nisin, which was purified according to Bonelli *et al.* [3]. Daptomycin, vancomycin, and sodium azide were dissolved in sterile water. Gramicidin ABCD, valinomycin, and benzyl alcohol were dissolved in sterile DMSO. Tunicamycin was dissolved in sterile DMF. If required, antibiotic concentrations were adjusted to the respective strains and growth conditions and are given in the figure legends.

Minimal inhibitory concentration (MIC) and growth curves

MICs were determined in Luria Bertani (LB) broth supplemented with 1.25 mM $CaCl_2$ in a standard serial dilution assay. Medium was inoculated with $5x10^5$ CFU/ml and incubated at 37 °C for 16 h. MIC was taken as lowest compound concentration inhibiting visible growth. For growth experiments cells were grown in LB with 1.25 mM $CaCl_2$ (and xylose, if appropriate) at 30 °C until an OD_{600} of 0.3 and subsequently treated with daptomycin. MICs and growth curves for determining the optimal concentration for proteome and element analysis were performed in Belitzky minimal medium (BMM) [4] at 37 °C in a tube assay as described previously [5].

Incorporation of radioactively labeled metabolic precursors

Incorporation of radiolabeled metabolic precursors ([^{14}C]-thymidine into DNA, [^{3}H]-glucosamine into cell wall, L-[^{14}C]-isoleucine into protein, and [^{3}H]-uridine into RNA) was performed as previously reported [6]. Briefly, *B. subtilis* 168 was grown at 37 °C in casein-yeast-glucose broth (CYG) supplemented with 50 mg/l $CaCl_2$ and 1 mM of the respective unlabeled metabolite. At an OD_{600} of 0.5, cultures were diluted to an OD_{600} of 0.04 and allowed to regrow to an OD_{600} of 0.4. The respective radiolabeled precursor was added to a final concentration of 1 µCi/ml, followed by addition of 3 µg/ml daptomycin, 0.3125 µg/ml ciprofloxacin, 0.3125 µg/ml rifampicin, 0.625 µg/ml vancomycin, or 10 µg/ml tetracycline (10xMIC in CYG). Untreated cultures were run as control. Macromolecules were precipitated with ice-cold 10% trichloroacetic acid containing 1 mM of unlabeled precursor and incubated for at least 30 minutes on ice before being filtered through glass microfiber filters (Whatman). Filters were washed with 5 ml 2.5% trichloroacetic acid containing 50 mM unlabeled metabolite and dried. Radioactivity was measured in a scintillation counter. Experiments were performed in biological and technical duplicates.

Proteomics

Proteome analysis was performed as described previously [5]. *B. subtilis* 168 (*trpC2*) [7] was grown at 37 °C under steady agitation in BMM. At an OD_{500} of 0.35 the main culture was split and either treated with 3.5 µg/ml daptomycin (50 % growth inhibition, Supplementary Figure 14) for 10 minutes or left untreated as control. Newly synthesized proteins were radioactively pulse-labeled by addition of 1 µCi/ml L-[^{35}S] methionine for additional 5 minutes. Incorporation was stopped by immediate transfer of cultures on ice and addition of 10 mM non-radioactive L-methionine and 1 mg/mL chloramphenicol. Sample preparation and analysis was performed as described before [5]. Crude protein extracts were separated in a first dimension by isoelectric focusing in a pI gradient from 4-7 and in a second dimension by SDS-PAGE. 2D gels were dried and autoradiographs were analyzed with Delta 2D image analysis software (Decodon) as described earlier [8]. Proteins found to be at least two-fold upregulated in three independent experiments were defined as marker proteins. Protein spots were excised from non-radioactive 2D gels, digested with trypsin, and identified by MALDI-ToF/ToF as described before [5].

Resazurin assay

Cells were grown in LB supplemented with 1.25 mM $CaCl_2$ at 30 °C until an OD_{600} of 0.3 and subsequently treated with 0.5, 1, 2, 4, or 8 mg/ml daptomycin, 1 µg/ml gramicidin ABCD, 100 µM CCCP, or 15 mM sodium azide. Samples were withdrawn after 5, 25, and 55 minutes, adjusted to an OD_{600} of 0.15 (dilution with medium), and incubated for 5 minutes with 100 µg/ml resazurin under steady agitation at 30 °C. Absorbance was measured at 540 and 630 nm. Experiments were performed in biological and technical duplicates.

ATP measurements

ATP levels were determined as described previously [9]. Cells were grown as for proteome analysis and treated with 3.5 µg/ml daptomycin, 10 µg/ml valinomycin, or 22.5 µg/ml MP196 for 15 minutes. ATP levels were measured in 100 µl cytosolic extracts using the ATPlite 1step kit (Perkin Elmer) following the manufacturer's instructions. Measurements were performed in quintuple biological and double technical replicates using the Infinite® 200 PRO multimode reader (Tecan).

Element analysis

Inductively-coupled plasma optical emission spectroscopy (ICP-OES) was performed under the same conditions used for proteomic profiling [9]. Only metal-free plastic ware and ultrapure water (Bernd Kraft) were used. Centrifugation steps were performed for 2 minutes in order to reduce sample handling time. *B. subtilis* 168 was grown in BMM to mid-log phase, washed twice in pre-warmed 100 mM Tris, 1 mM EDTA, pH 7.5, washed and resuspended in the same buffer without EDTA. Tris buffer constitutes an environment, where cells cannot compensate for ion fluxes. Under these conditions, even slightest effects that could not be measured under normal growth conditions become detectable [10]. Cell density was adjusted to an OD_{500} of 0.4 prior to addition of 3.5 µg/ml daptomycin or 10 µg/ml valinomycin. After 5 minutes of treatment cells were harvested, digested in nitric acid, and subjected to element analysis. Element concentrations were determined by ICP-OES using an iCAP* 6300 Duo View ICP Spectrometer (Thermo Fisher Scientific)[9]. Element concentrations were converted into intracellular ion concentrations based on calculation of the cytosolic volume of *B. subtilis*. This volume was taken as 3.09×10^{-9} µl based on average rod size and *B. subtilis* cell wall and membrane thickness determined by cryo-electron microscopy by Matias and Beveridge [11,12]. Experiments were performed in biological triplicates and technical duplicates.

Determination of the membrane potential

The membrane potential levels were determined for *B. subtilis* cells as described earlier [13] with following modifications. Cells were grown in LB supplemented with 1.25 mM $CaCl_2$ to an OD_{600} of 0.35 at 30 °C, followed by determination of membrane potential levels directly in the growth medium. Measurements were carried out in black polystyrene microtiter plates (Labsystems) using BMG Fluostar Optima fluorimeter equipped with 610±5 nm excitation, and 660±5 nm emission filters. As a positive control, membrane potential was dissipated with gramicidin ABCD (2 µM). Experiments were performed in biological duplicates and technical triplicates.

Laurdan-based membrane fluidity measurements

Determination of membrane fluidity by laurdan generalized polarization (GP) was performed as described previously [14] with some modifications. *B. subtilis* was grown in LB supplemented with 1.25 mM $CaCl_2$ and 0.2% glucose at 30 °C. At an OD_{600} of 0.35 cells were stained with 10 µM laurdan for 5 minutes. Laurdan was dissolved in DMF and a final concentration of 1% DMF was maintained in the medium for better solubility. Cells were washed four times with pre-warmed PBS supplemented with 0.2% glucose prior to addition of antibiotics (1, 2, or 4 µg/ml daptomycin, 2 µg/ml gramicidin ABCD) and were further incubated under steady agitation. Laurdan fluorescence intensities were measured at 460±5 nm and 500±5 nm upon excitation at 330±5 nm using BMG Fluostar Optima fluorimeter at 30 °C. Laurdan GP was calculated using the formula GP = (I460-I500)/(I460+I500). For endpoint determination of membrane fluidity after long-term treatment, samples were taken before and after 30, 60, and 90 minutes of treatment, stained, washed, and measured as described above. Fluidity measurements were performed in biological duplicates and technical triplicates.

Microscopy

Overnight cultures were grown at 30 °C in LB supplemented with 1.25 mM $CaCl_2$ and appropriate inducer concentrations (Supplementary Table 2). Cells were diluted 100-fold in the same medium and grown at 30 °C until an OD_{600} of 0.3. Cultures were then split and treated with daptomycin (1 or 2 µg/ml) or left untreated as control. Samples were immobilized on microscope slides covered with a 1.2% agarose film and imaged immediately. Fluorescence microscopy was carried out using a Zeiss Axiovert 200M equipped with a Zeiss Neofluar 100x /1.30 Oil Ph3 objective, a Lambda S light source (Shutter Instruments), a Photometrics Coolnap HQ2 camera, and Metamorph 6 software (Molecular Devices) (Figure 3) or a Nikon Eclipse Ti equipped with a CFI Plan Apochromat DM 100x oil objective, an Intensilight HG 130

W lamp, a C11440-22CU Hamamatsu ORCA camera, and NIS elements software, version 4.20.01 (all other figures). Images were analyzed using ImageJ (National Institutes of Health) v.1.38 or v.1.48.

Propidium iodide-based pore stain was performed with the Live/Dead bacterial viability kit (Invitrogen) as described earlier [15]. Membranes were stained with 2 µg/ml FM5-95 (Molecular Probes) for 5 minutes immediately prior to microscopy. For RIF staining with DiIC12 (Anaspec) overnight cultures were diluted 1:200 in LB containing 1.25 mM $CaCl_2$, 1% DMSO, 2 µg/ml DiIC12, and inducer where appropriate, and grown until an OD_{600} of 0.3. Cells were washed four times and resuspended in the same medium without DiIC12 (pre-warmed to 30 °C) followed by daptomycin treatment. Labeling of daptomycin with the fluorescent Bodipy-FL (Molecular Probes, Invitrogen) was performed by incubating 10 mg of the antibiotic with the amine-reactive STP ester (solubilized in DMSO) in 0.1 M sodium bicarbonate buffer, pH 8.3, at room temperature under continuous mixing, according to the manufacturer's instructions. Unbound conjugate was removed by extensive dialysis against bicarbonate buffer. Although the labeled compound was 8-fold less active in terms of MIC, concentrations comparable to unlabeled daptomycin (3 µg/ml compared to 1-2 µg/ml of unlabeled compound) were sufficient to cause the same phenotype in log phase cells (elongation and membrane patches that overlap with daptomycin-Bodipy foci). Therefore, we concluded that labeling of daptomycin with Bodipy does not profoundly change its mechanism. For co-localization of daptomycin-Bodipy with DiIC12, DiIC12-stained cell suspensions were mixed with 3 µg/ml of labeled and 1 µg/ml of unlabeled daptomycin and incubated for 10 minutes in LB containing 1.25 mM $CaCl_2$ and 1% DMSO, followed by washing and resuspension in the same medium to remove excess daptomycin-Bodipy and reduce background fluorescence. For daptomycin-Bodipy co-localization with DiIC12 in cells pre-treated with benzyl alcohol, this washing step was omitted in order not to remove the benzyl alcohol.

Microscopic measurement of membrane fluidity was performed as described before [14]. Briefly, *B. subtilis* was grown in LB supplemented with 1.25 mM CaCl2 until an OD_{600} of 0.35, incubated for 5 minutes with 100 µM laurdan (final concentration of 1% DMF), washed and resuspended in PBS, and immediately used for fluorescence microscopy at 30 °C using temperature-controlled Applied Precision DeltaVision RT microscope. Laurdan was exited at 360 ± 20 nm and fluorescence emission was captured at 528 ± 19 nm followed by a second image at 457 ± 25 nm. Image analysis and generation of a color-coded generalized polarization (GP) maps was performed with Wolfram Mathematica 7 (Wolfram Research). All microscopy experiments were performed in at least two biological replicates.

Supporting Table 1: *B. subtilis* strains used in this study. gfp: green fluorescent protein, mgfp: monomeric gfp, sfgfp: superfolder gfp, msfgfp: monomeric superfolder gfp, MCS: multiple cloning site

Strain	genotype	induction	reference
168	*trpC2*	-	[7]
JWV042	*amyE::cat Phbs-hbs-gfp*	-	[13]
HM160	*kan spo0J-gfp*	-	[13]
PolC-GFP	*amyE::spc Pxyl-polC-gfp*	0.1% xylose	[16]
1049	*amyE::spc Pxyl-rpsB-gfp*	1% xylose	[17]
1048	*cat rpoC-gfp Pxyl-‘rpoC*	1% xylose	[17]
YK405	*amyE::spc Pxyl-gfp-mreB*	-	[18]
MW10	*amyE::spc Pxyl-gfp-mreB* (YK405 transformed to 168)	0.3% xylose	this study
3417	*cat mreC::Pxyl-gfp-mreC*	0.3% xylose	[19]
3416	*cat mreC::Pxyl-gfp-mreD*	0.3% xylose	[19]
2020	*aprE::spc Pspac-gfp-ftsZ*	0.1 mM IPTG	[20]
PG62	*aprE::spc Pspac-yfp-ftsA*	0.1 mM IPTG	[21]
1981	*amyE::spc Pxyl-gfp-minD*	-	[22]
LH131	*amyE::spc Pxyl-gfp-minD* (1981 transformed to 168)	0.1% xylose	this study
HS63	*amyE::spc Pxyl-divIVA-msfgfp*	0.5% xylose	[23]
BMK21	*amyE::scp Pxyl-divIVA-sfgfp*	0.5% xylose	this study
BS23	*atpA-gfp Pxyl-’atpA cat*	0.1% xylose	[24]
4277	*Ωneo3427 ΔmreB Δmbl::cat ΔmreBH::erm ΔrsgI::spc*	-	[25]
TNVS29D	*amyE::spc-Pxyl-mgfp-plsX*	0.5% xylose	this study
TNVS45	*amyE::spc-Pxyl-mgfp-ponA*	0.1% xylose	this study
TNVS175	*amyE::spc-Pxyl-murG-msfgfp*	0.05% xylose	this study
TNVS183	*murG::murG msfgfp-Pspac-murB ery*	0.1 mM IPTG	this study
TNVS284	*amyE::spc-Pxyl-mraY-msfgfp*	0.1% xylose	this study
EKB44	*amyE::spc-Pxyl-msfgfp-pbpB*	0.1% xylose	this study

Supporting Table 2: Plasmids used in this study

plasmid	genotype	source
pSG1729	*amyE3': spc- Pxyl-gfp-MCS-amyE5' bla* (N-terminal fusion)	[26]
pHJS103	*amyE3': spc- Pxyl-sfgfp-MCS-amyE5' bla* (N-terminal fusion)	this study
pHJS105	*amyE3': spc- Pxyl-msfgfp-MCS-amyE5' bla* (N-terminal	[23]
pDG7-sfGFP	*amyE3': spc-Pxyl-divIVA-sfgfp-amyE5' bla* (pDG7 with *sfgfp*)	[27]
pDG7-msfGFP	*amyE3': spc-Pxyl-divIVA-msfgfp-amyE5' bla*	this study
pEKC12	*amyE3': spc- Pxyl-msfgfp-pbpB-amyE5' bla*	this study
pMW1	*amyE3': spc- Pxyl-msfgfp-MCS-amyE5' bla* (C-terminal	this study
pSG1154	*amyE3': spc- Pxyl-mgfp-MCS-amyE5' bla*	[26]
pTNV12	*amyE3': spc*-Pxyl-*mgfp-plsX-amyE5' bla*	this study
pTNV20	*amyE3': spc*-Pxyl-*mgfp-ponA-amyE5' bla*	this study
pTNV64	*amyE3': spc-Pxyl-msfgfp-amyE5' bla*	this study
pTNV77	*amyE3': spc-Pxyl-murG-msfgfp-amyE5' bla*	this study
pTNV81	*pMUTIN-murG(G193-K363)-msfgfp bla ery*	this study
pTNV105	*amyE3': spc-Pxyl-mraY-msfgfp-amyE5' bla*	this study

Supporting Table 3: Primers used in this study

primer	sequence
EKP20	TAAATGTCCAGACTTCAGATCCAC
EKP30	GTGGATCCGAAGTCTGGACATTTT
EKP31	TGTCCAGACTTCGGATCCACatgATTCAAATGCCAAAAAA
EKP32	ATCAAGCTTATCGATACCGTCGACttaATCAGGATTTTTA
GFPA206K-for	CCTGTCCACACAATCTAAACTTTCGAAAGATCCC
GFPA206K-rev	GGGATCTTTCGAAAGTTTAGATTGTGTGGACAGG
HS404	CCTGTCGACACAATCTAAACTTTCGAAAGATCCC
HS405	GGGATCTTTCGAAAGTTTAGATTGTGTCGACAGG
MW30	GAGCTCTACAAATAGATGTCCAGACTTCAGATCCACTAGT
MW31	CAGGGTACCCATCTGCAGGAATTCGATATCAAGCT
MW32	GAATTCCTGCAGATGGGTACCCTGCAGATGAGC
MW33	CTGAAGTCTGGACATCTATTTGTAGAGCTCATCCATGCCATG
PlsX-Fw	GGGCTCGAGGGCTCAGGAAGCGGCTCAGGATCCAGAATAGCTGTAGATGCAATG
PlsX-Re	CCCCGGCCGCTACTCATCTGTTTTTTCTTCTTTCAC
TerS93	GGGGCTCGAGGGCTCAGGAAGCGGCTCAGGATCCATGTCAGATCAATTTAACAGCCGTG
TerS94	CCCGAATTCTTAATTTGTTTTTCAATGGATGATGA
TerS145	ATAAACAAATAGGGGTTCCGCGCA
TerS146	TGCGCGGAACCCCTATTTGTTTAT
TerS273	AGCAAAGGAGAAGAACTTTTCACTGGAGT
TerS277	TCTAGATGCATTTTATGTCATATTGT
TerS278	AAAAGTTCTTCTCCTTTGCTCTGCAGGAATTCGATATCAAGCT
TerS340	GCGTCAGCGTGTAAATTCCGTCT
TerS343	CGGAATTTACACGCTGACGCTGCCT
TerS366	GGATCCTGAGCCGCTTCCTGAGCCGGATCCTGAGCCGCTTCCTGAGCCTTTTTTTAATTCC TCGAGTACGCT
TerS367	TGACATAAAATGCATCTAGAGGGTTATCGTTATGTTATAGAGA
TerS368	GGCTCAGGAAGCGGCTCAGGATCCAAAGGAGAAGAACTTTTCACTGGAGT
TerS369	TAATAATAACCGGGCAGGCCATGTCT
TerS370	CCCTATATAAAAGCATTAGTGTATCA
TerS371	ACTAATGCTTTTATATAGGGCGGCGGTAAGCCGAGGCGCTGCA
TerS372	GGCCTGCCCGGTTATTATTACTATTTGTAGAGCTCATCCATGCCA
TerS403	TAGATGTCCAGACTTCAGATCCA
TerS404	CCTGAGCCGCTTCCTGAGCCTAACCACACCTCGATGTAAATTCCT
TerS405	TGACATAAAATGCATCTAGAGAATATGATAACTACGTATGTCGT

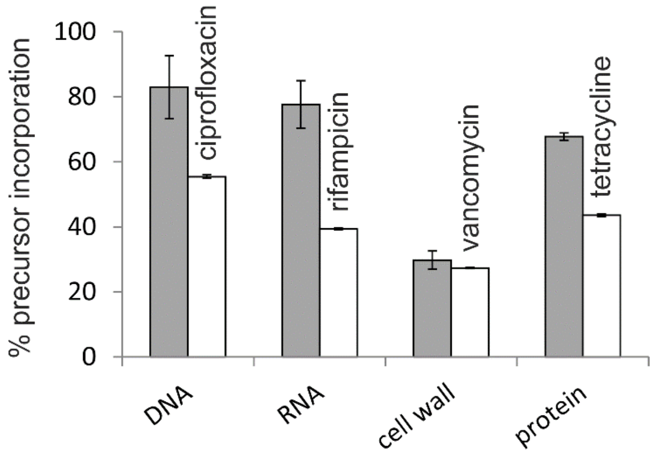

Supporting Figure 1: Effect of daptomycin on macromolecule synthesis. Incorporation of ^{14}C-thymidine (DNA), ^{3}H-uridine (RNA), ^{14}C -isoleucine (protein), and ^{3}H-glucosamine (cell wall) was determined in cells treated with daptomycin(grey bars). Ciprofloxacin, rifampicin, vancomycin and tetracycline were used as control antibiotics. The amount of radiolabeled precursors incorporated in untreated control cells was taken as 100%. Error bars represent standard deviation of the mean.

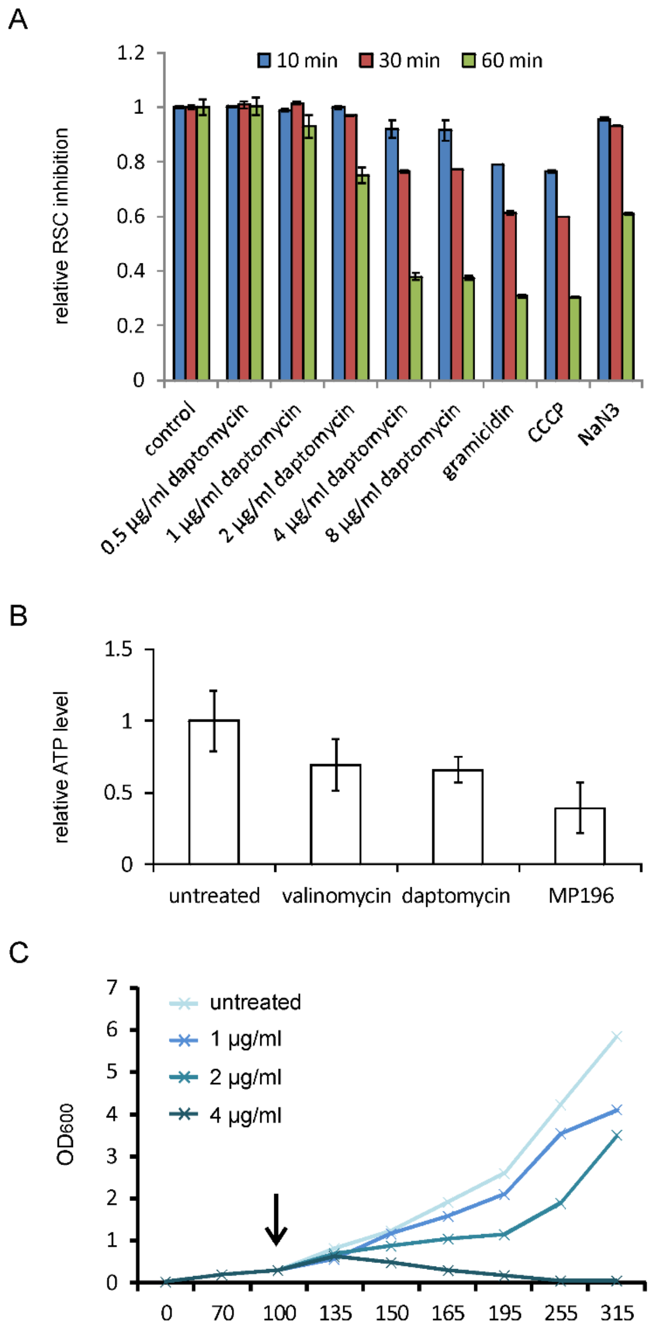

Supporting Figure 2: Effects of daptomycin on energy metabolism and cell growth. (**A**) Effect on respiratory chain activity measured by reduction of blue resazurin (630 nm) to red resorufin (540 nm). (**B**) Effect on ATP concentrations measured with a luciferase-based assay and expressed relative to the untreated control. Cells were grown and treated as described for proteome analysis in the main text (3.5 µg/ml daptomycin). Error bars represent standard deviations of the mean. (**C**) Growth curves of cells in LB medium supplemented with 1.25 mM $CaCl_2$ and exposed to different daptomycin concentrations at OD_{600} ~0.3 (arrow).

Supporting Figure 3: Cell permeability assay using propidium iodide. *B. subtilis* 168 was grown under the same conditions described for proteomic conditions (3.5 µg/ml daptomycin). Green fluorescence (SYTO9) indicates cells with intact membranes while red fluorescence (propidium iodide) indicates the presence of membrane pores [15]. Nisin is used as positive control. Clearly, under these conditions daptomycin does not form pores in the membrane. Field width 6 µm.

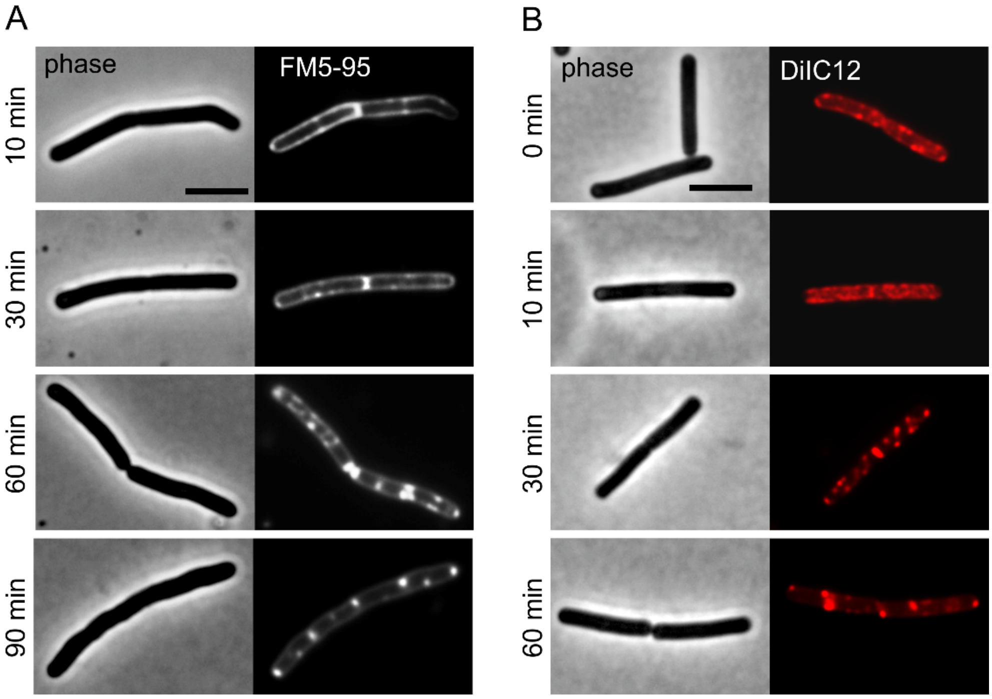

Supporting Figure 4: Effect on membrane lipids. **(A)** Visibility of lipid patches stained with FM5-95 over time. **(B)** Organization of fluid lipid domains stained with DiIC12. *B. subtilis* 168 was grown at 30 °C in LB + 1.25 mM $CaCl_2$ until an OD_{600} of ~0.3 prior to antibiotic treatment. Note that membrane patches become visible with the fluid lipid domain dye DiIC12 before they appear with the unselective FM5-95 stain. Scale bars represent 2 µm.

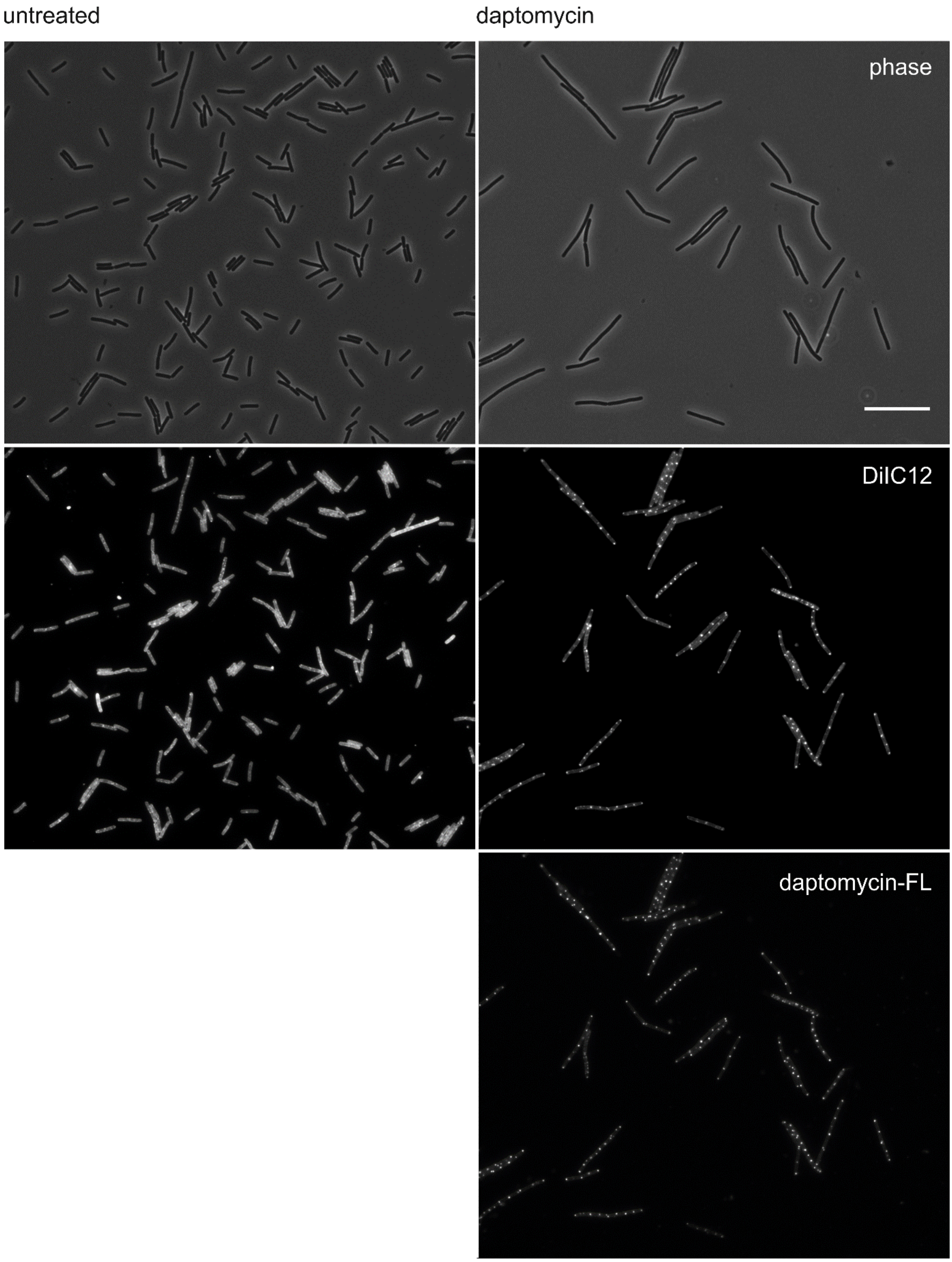

Supporting Figure 5: Overview pictures of DiIC12-stained membrane patches. *B. subtilis* 168 was grown in LB supplemented with 1.25 mM $CaCl_2$ until an OD_{600} of 0.3. Cells were treated with 3 µg/ml daptomycin-BODIPY and 1 µg/ml unlabeled daptomycin. Scale bar 10 µm

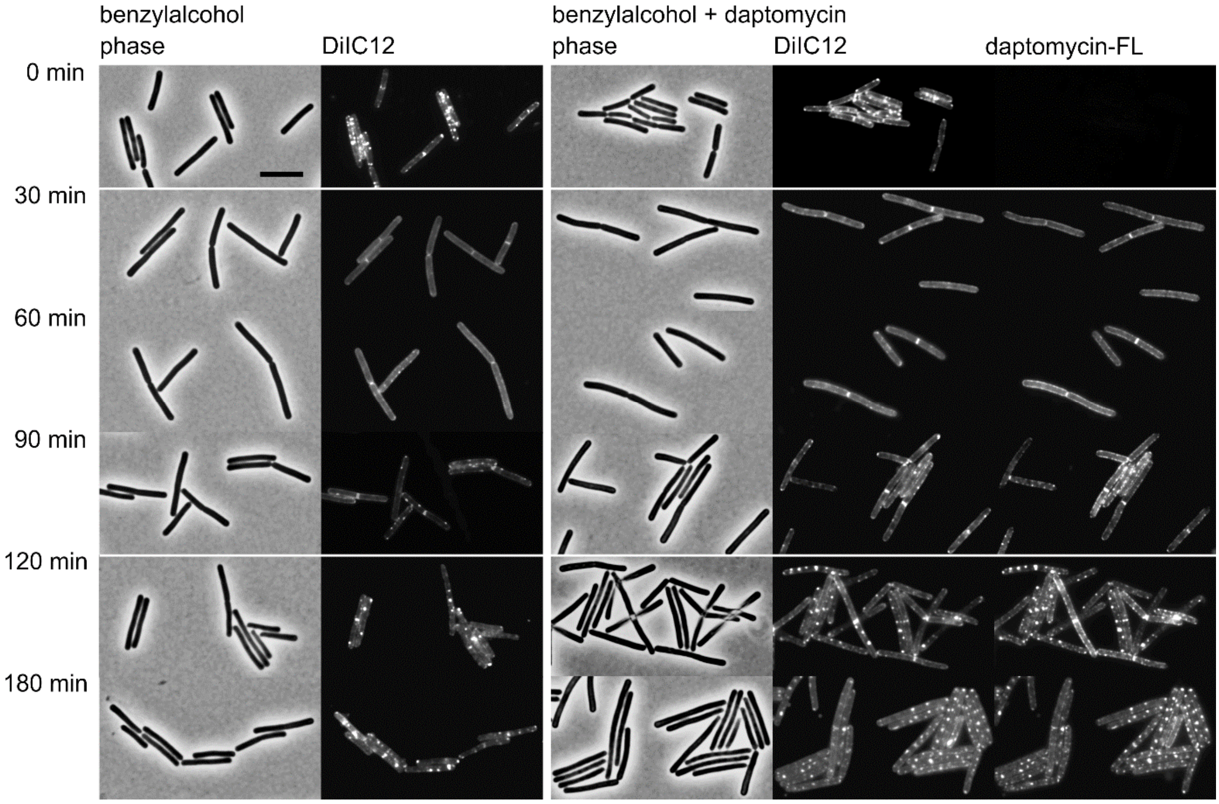

Supporting Figure 6: Overview pictures of co-localization of DiIC12 with daptomycin-BODIPY in cells pre-treated with benzyl alcohol. *B. subtilis* 168 was grown in LB supplemented with 1.25 mM $CaCl_2$ until an OD_{600} of 0.3. Cells were treated with 50 mM benzyl alcohol for 10 minutes prior to addition of 3 µg/ml daptomycin-BODIPY and 1 µg/ml unlabelled daptomycin. Addition of benzyl alcohol diminishes RIFs in the *B. subtilis* membrane, rendering daptomycin unable to form clusters and preventing fluid lipid clustering. However, the effect of benzyl alcohol on membrane organization is transient. Cells recover fluid domains after 90 minutes and in cells pre-treated with benzylalcohol, both clustering of daptomycin and concomitant forming of lipid domains is not prevented completely but delayed by 90 minutes. Scale bar 4 µm.

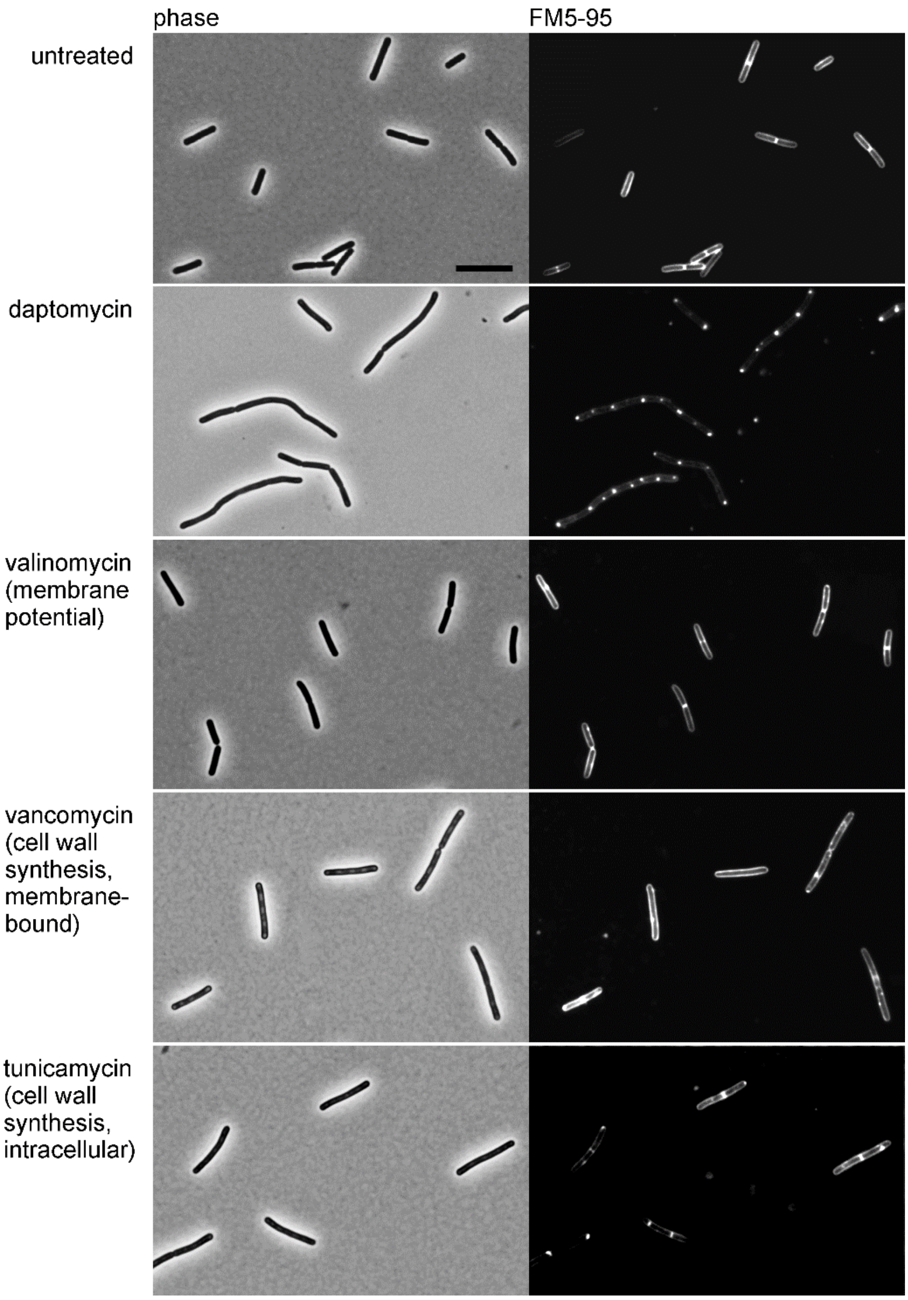

Supporting Figure 7: Overview of the effects of different cell envelope-targeting antibiotics on the membrane of *B. subtilis*. *B. subtilis* 168 was grown at until an OD_{600} of 0.3 and treated with 2 µg/ml daptomycin (grown in LB + 1.25 mM $CaCl_2$), 10 µg/ml valinomycin (grown in TY + 300 mM KCl), 2 µg/ml vancomycin, or 3 µg/ml tunicamycin (grown in LB + 1.25 mM $CaCl_2$). Pictures were taken after 90 minutes of treatment. Scale bar 5 µm.

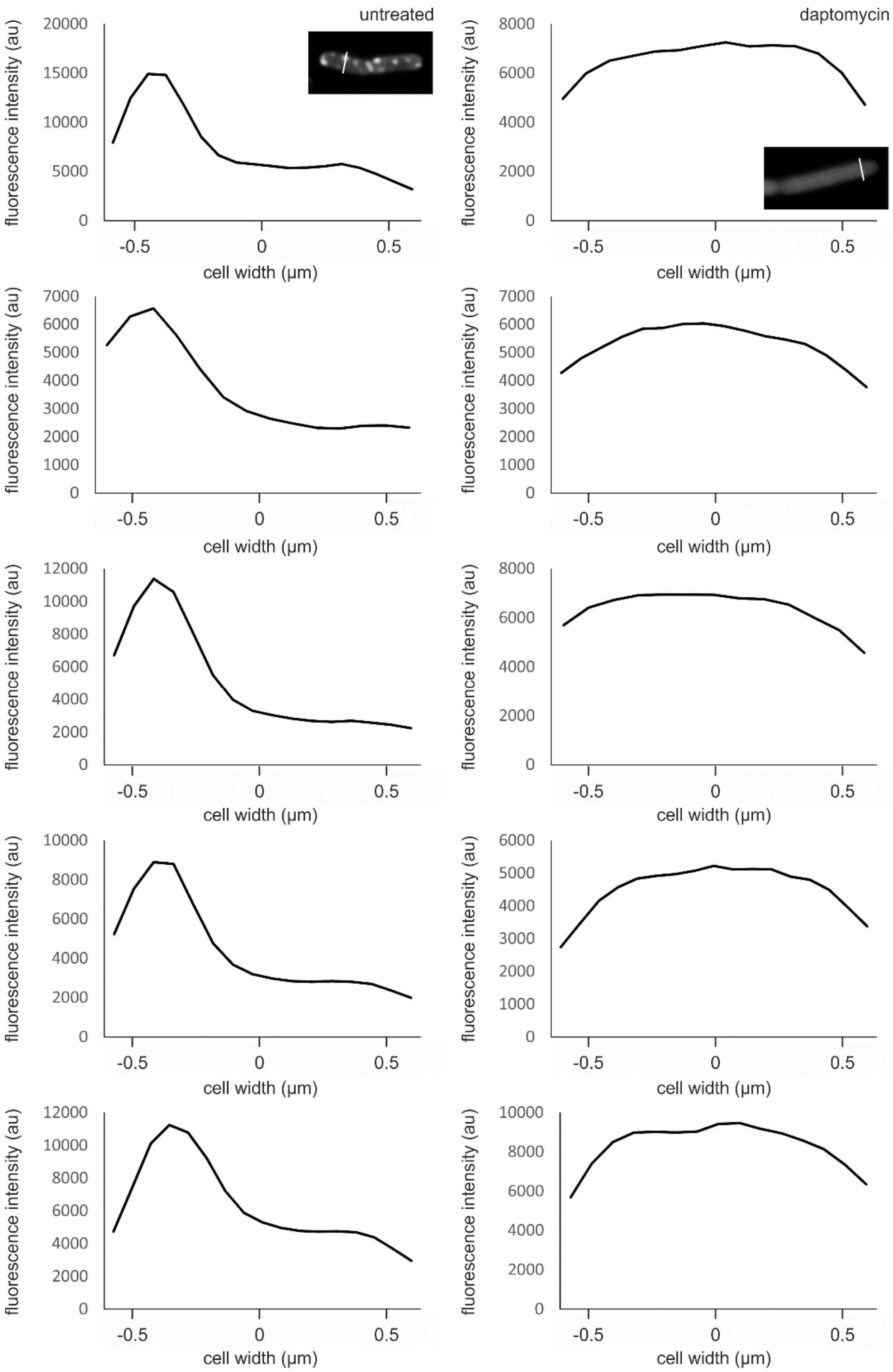

Supporting Figure 8: Line scans of 5 representative cells expressing MurG-GFP before and after 10 minutes treatment with 2 µg/ml daptomycin. Microscopy pictures show how line scans were performed.

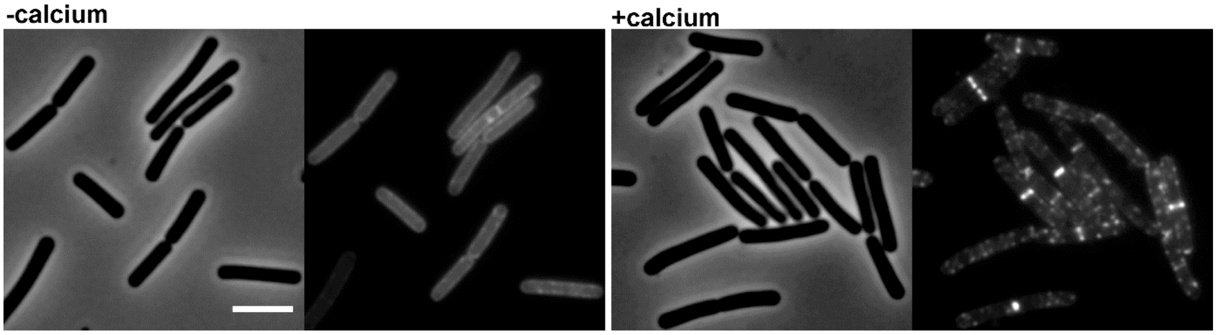

Supporting Figure 9: *B. subtilis* after 10 minutes treatment with 1 µg/ml daptomycin and 3 µg/ml daptomycin-Bodipy in the absence and presence of 1.25 mM $CaCl_2$.

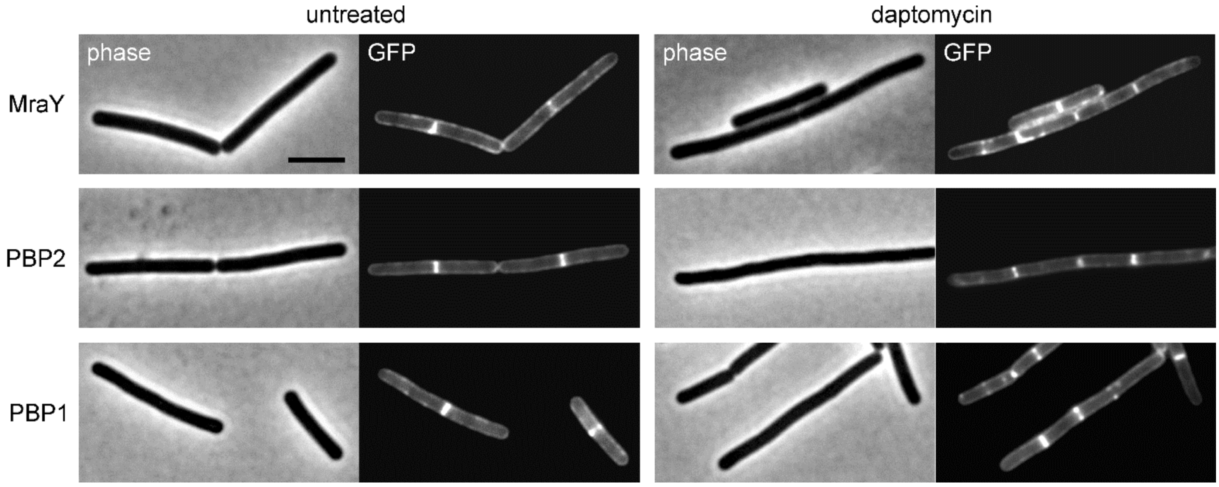

Supporting Figure 10: Daptomycin does not influence the membrane localization of the cell wall synthesis proteins MraY, PBP1 (*ponA*), and PBP2 (*pbpB*). *B. subtilis* TNVS284 (*mraY-msfgfp*), EKB44 (*msfgfp-pbpB*), and TNVS45 (*msfgfp-ponA*) were grown in LB supplemented with 1.25 mM $CaCl_2$ until an OD_{600} of 0.3 and treated with 2 µg/ml daptomycin for 30 minutes. Scale bar 2 µm.

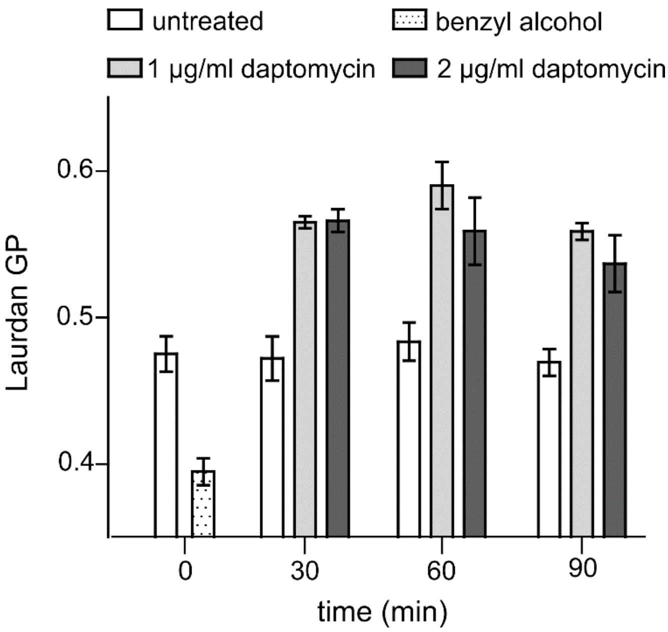

Supporting Figure 11: Membrane fluidity after prolonged daptomycin treatment. *B. subtilis* 168 was grown in LB supplemented with 1.25 mM $CaCl_2$ until OD 0.3 and treated with 50 mM benzyl alcohol or 1 or 2 µg/ml daptomycin. Error bars represent standard deviations of the mean.

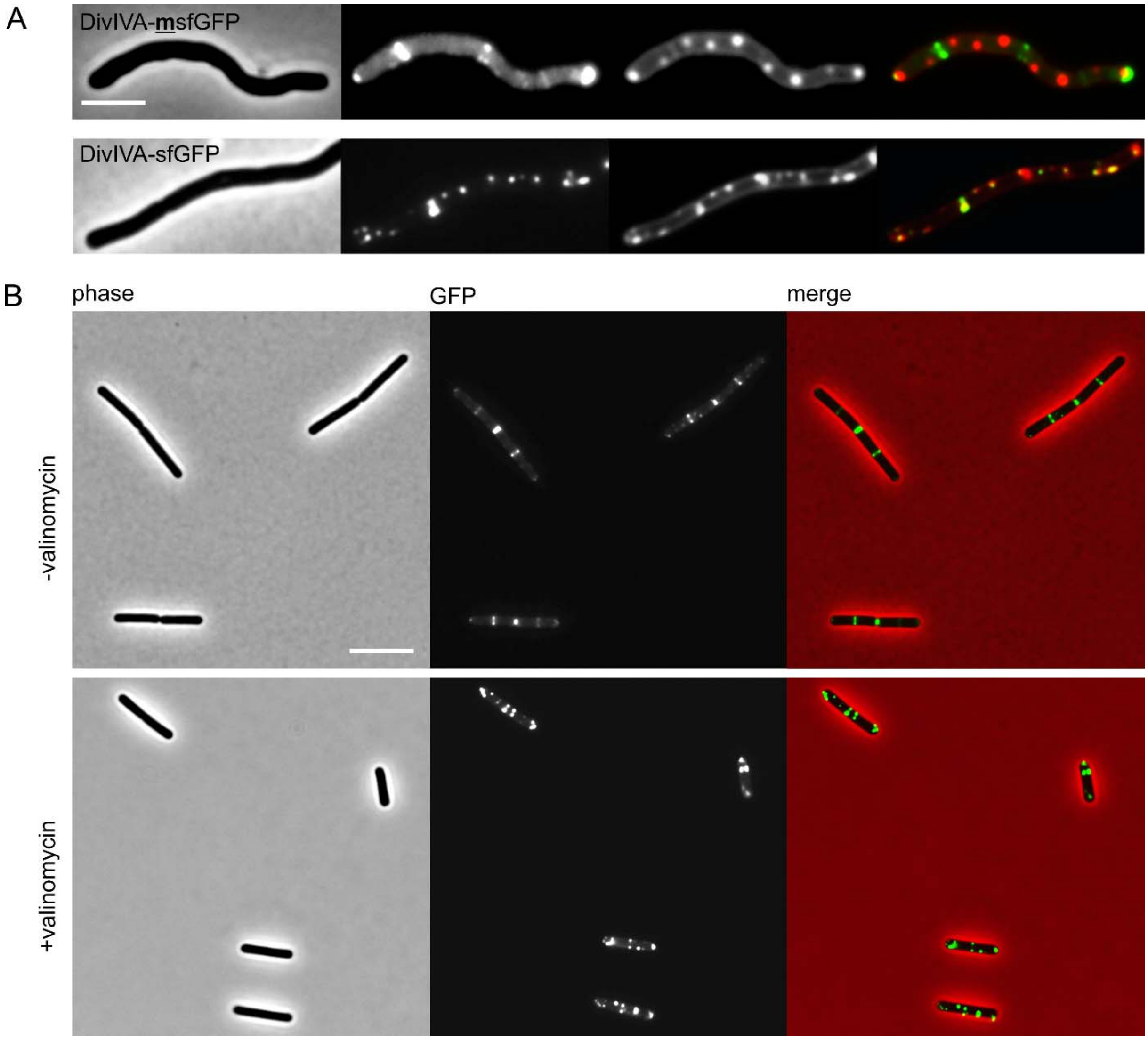

Supporting Figure 12: Localization of DivIVA. **(A)** DivIVA fused to monomeric sfGFP does not co-localize with lipid patches (upper panel) while an old non-monomeric sfGFP fusion to DivIVA is attracted to membrane patches caused by daptomycin (lower panel). Scale bar 2 µm. **(B)** Localization of DivIVA fused to monomeric GFP is sensitive for the membrane potential. Scale bar 3 µm. *B. subtilis* HS63 (*divIVA-msfgfp*) and BMK21 (*divIVA-sfgfp*) were grown in LB with 300 mM KCl in the presence of 0.5% xylose to induce the fusion protein, and treated with 10 µg/ml valinomycin at an OD_{600} of 0.3 to dissipate the membrane potential. Pictures were taken after 15 minutes. Scale bar 3 µm.

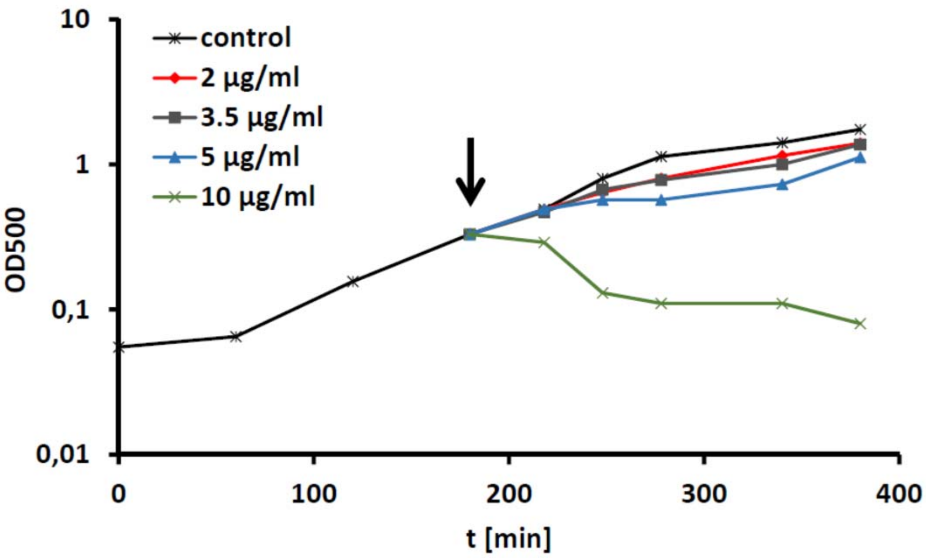

Supporting Figure 13: Growth experiments for proteome analysis. *B. subtilis* 168 was grown in BMM (MIC 2 µg/ml) until mid-log phase. Then the culture was split and treated with different antibiotic concentrations to find an optimal stressor concentration that inhibits growth but still allows active protein biosynthesis (~50% reduced growth rate). 3.5 µg/ml daptomycin was used for proteomics and follow up experiments. Arrow indicates time point of antibiotic addition.

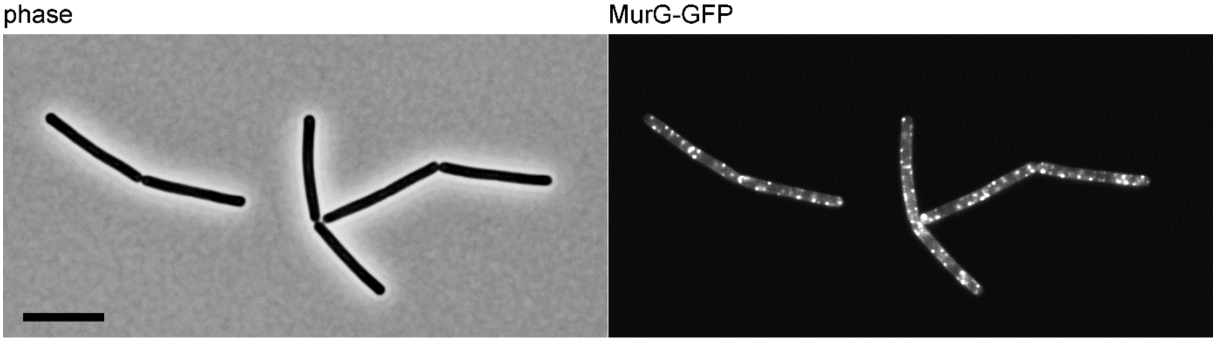

Supporting Figure 14: MurG-msfGFP is functional. *murG-msfGFP* was integrated into the *murG* locus, thereby disrupting the native *murG* gene (TNVS183). MurG-msfGFP is expressed from the native *murG* promoter and downstream genes are driven by *Pspac* using 0.1 mM IPTG. Cells were viable and MurG showed the same localization pattern as observed with the xylose-inducible *murG-msfGFP* construct. Scale bar 4 µm.

References

1. Gibson, D. G. *et al.* Enzymatic assembly of DNA molecules up to several hundred kilobases. *Nat Meth* **6,** 343–345 (2009).
2. Hauser, P. M. & Karamata, D. A rapid and simple method for Bacillus subtilis transformation on solid media. *Microbiology* **140,** 1613–1617 (1994).
3. Bonelli, R. R., Schneider, T., Sahl, H.-G. & Wiedemann, I. Insights into in vivo activities of lantibiotics from gallidermin and epidermin mode-of-action studies. *Antimicrob. Agents Chemother.* **50,** 1449–1457 (2006).
4. Stülke, J., Hanschke, R. & Hecker, M. Temporal activation of beta-glucanase synthesis in Bacillus subtilis is mediated by the GTP pool. *J. Gen. Microbiol.* **139,** 2041–2045 (1993).
5. Wenzel, M. *et al.* Proteomic signature of fatty acid biosynthesis inhibition available for in vivo mechanism-of-action studies. *Antimicrob. Agents Chemother.* **55,** 2590–2596 (2011).
6. Schneider, T. *et al.* In vitro assembly of a complete, pentaglycine interpeptide bridge containing cell wall precursor (lipid II-Gly5) of Staphylococcus aureus. *Mol. Microbiol.* **53,** 675–685 (2004).
7. Anagnostopoulos, C. & Spizizen, J. Requirements for transformation in Bacillus subtilis. *J. Bacteriol.* **81,** 741–746 (1960).
8. Bandow, J. E. *et al.* Improved image analysis workflow for 2-D gels enables large-scale 2-D gel-based proteomics studies--COPD biomarker discovery study. *Proteomics* **8,** 3030–3041 (2008).
9. Wenzel, M. *et al.* Small cationic antimicrobial peptides delocalize peripheral membrane proteins. *Proc. Natl. Acad. Sci. U. S. A.* **111,** E1409–18 (2014).
10. Wenzel, M. *et al.* Antimicrobial Peptides from the Aurein Family Form Ion-Selective Pores in Bacillus subtilis. *ChemBioChem* **16,** 1101–08 (2015).
11. Matias, V. R. F. & Beveridge, T. J. Lipoteichoic acid is a major component of the Bacillus subtilis periplasm. *J. Bacteriol.* **190,** 7414–7418 (2008).
12. Matias, V. R. F. & Beveridge, T. J. Cryo-electron microscopy reveals native polymeric cell wall structure in Bacillus subtilis 168 and the existence of a periplasmic space. *Mol. Microbiol.* **56,** 240–251 (2005).
13. Strahl, H. & Hamoen, L. W. Membrane potential is important for bacterial cell division. *Proc. Natl. Acad. Sci. U. S. A.* **107,** 12281–12286 (2010).
14. Strahl, H., Burmann, F. & Hamoen, L. W. The actin homologue MreB organizes the bacterial cell membrane. *Nat. Commun.* **5,** 3442 (2014).
15. Wenzel, M. *et al.* Analysis of the mechanism of action of potent antibacterial hetero-tri-organometallic compounds: A structurally new class of antibiotics. *ACS Chem. Biol.* **8,** 1442–1450 (2013).
16. Migocki, M. D., Lewis, P. J., Wake, R. G. & Harry, E. J. The midcell replication factory in Bacillus subtilis is highly mobile: implications for coordinating chromosome replication with other cell cycle events. *Mol. Microbiol.* **54,** 452–463 (2004).
17. Lewis, P. J., Thaker, S. D. & Errington, J. Compartmentalization of transcription and translation in Bacillus subtilis. *EMBO J.* **19,** 710–718 (2000).
18. Kawai, Y., Daniel, R. A. & Errington, J. Regulation of cell wall morphogenesis in Bacillus subtilis by recruitment of PBP1 to the MreB helix. *Mol. Microbiol.* **71,** 1131–1144 (2009).
19. Leaver, M. & Errington, J. Roles for MreC and MreD proteins in helical growth of the cylindrical cell wall in Bacillus subtilis. *Mol. Microbiol.* **57,** 1196–1209 (2005).
20. Stokes, N. R. *et al.* Novel inhibitors of bacterial cytokinesis identified by a cell-based antibiotic screening assay. *J. Biol. Chem.* **280,** 39709–39715 (2005).
21. Gamba, P., Veening, J. W., Saunders, N. J., Hamoen, L. W. & Daniel, R. A. Two-step assembly dynamics of the Bacillus subtilis divisome. *J. Bacteriol.* **191,** 4186–4194 (2009).
22. Marston, A. L., Thomaides, H. B., Edwards, D. H., Sharpe, M. E. & Errington, J. Polar

localization of the MinD protein of Bacillus subtilis and its role in selection of the mid-cell division site. *Genes Dev.* **12,** 3419–3430 (1998).
23. Jahn, N., Brantl, S. & Strahl, H. Against the mainstream: the membrane-associated type I toxin BsrG from Bacillus subtilis interferes with cell envelope biosynthesis without increasing membrane permeability. *Mol. Microbiol.* **98,** 651–666 (2015).
24. Johnson, A. S., van Horck, S. & Lewis, P. J. Dynamic localization of membrane proteins in Bacillus subtilis. *Microbiology* **150,** 2815–2824 (2004).
25. Schirner, K. & Errington, J. The cell wall regulator {sigma}I specifically suppresses the lethal phenotype of mbl mutants in Bacillus subtilis. *J. Bacteriol.* **191,** 1404–1413 (2009).
26. Lewis, P. J. & Marston, A. L. GFP vectors for controlled expression and dual labelling of protein fusions in Bacillus subtilis. *Gene* **227,** 101–110 (1999).
27. Lenarcic, R. *et al.* Localisation of DivIVA by targeting to negatively curved membranes. *EMBO J.* **28,** 2272–2282 (2009).